Plant Physiology and Biochemistry 142 (2019) 415–428

Contents lists available at ScienceDirect

Plant Physiology and Biochemistry

journal homepage: www.elsevier.com/locate/plaphy

Research article

Comparative transcriptomics and weighted gene co-expression correlation network analysis (WGCNA) reveal potential regulation mechanism of carotenoid accumulation in *Chrysanthemum* × *morifolium*

Chenfei Lu[a,b,c,d,1], Ya Pu[a,b,c,d,1], Yuting Liu[a,b,c,d], Yajun Li[a,b,c,d], Jiaping Qu[a,b,c,d], He Huang[a,b,c,d,*], Silan Dai[a,b,c,d,**]

[a] Beijing Key Laboratory of Ornamental Plants Germplasm Innovation & Molecular Breeding, Beijing, 100083, China
[b] National Engineering Research Center for Floriculture, Beijing, 100083, China
[c] Beijing Laboratory of Urban and Rural Ecological Environment, Beijing, 100083, China
[d] College of Landscape Architecture, Beijing Forestry University, Beijing, 100083, China

ARTICLE INFO

Keywords:
Carotenoids
Proplastids
Chloroplasts
Chromoplasts
Ultrastructures
Chrysanthemum
WGCNA

ABSTRACT

The variation of flower color of chrysanthemum (*Chrysanthemum*×*morifolium*) is extremely rich, and carotenoids, which are mainly stored in the plastid, are important pigments that determine the color of chrysanthemum. However, the genetic regulation of the carotenoid metabolism pathway in this species still remains unclear. In this study, a pink chrysanthemum cultivar, 'Jianliuxiang Pink', and its three bud sport mutants (including white, yellow and red color mutants, 'Jianliuxiang White', 'Jianliuxiang Yellow' and 'Jianliuxiang Red', respectively) were used as experimental materials to analyze the dynamic changes of carotenoid components and plastid ultrastructure at different developmental stages of ray florets. We found that the carotenoid components and plastid ultrastructure of the four color cultivars in the early developmental stage of the chrysanthemum capitulum (S1) were almost identical, and the carotenoids mainly included violaxanthin, lutein and β-carotene, which exist in proplastids and immature chloroplasts. With the development of capitulum, the chloroplasts in 'Jianliuxiang White' and 'Jianliuxiang Pink' were degraded, and the protoplasts did not transform but rather formed vesicles that accumulated trace amounts of carotenoids. The proplastids and chloroplasts in 'Jianliuxiang Yellow' and 'Jianliuxiang Red' were all transformed into chromoplasts and consist of lutein as well as lutein's isomer and derivatives. Using comparative transcriptomics combined with gene expression analysis, we found that *CmPg-1, CmPAP10,* and *CmPAP13*, which were involved in chromoplast transformation, *CmLCYE*, which was involved in carotenoid biosynthesis, and *CmCCD4a-2*, which was involved in carotenoid degradation, were differentially expressed between four cultivars, and these key genes therefore should affect the accumulation of carotenoids in chrysanthemum. In addition, six transcription factors, *CmMYB305, CmMYB29, CmRAD3, CmbZIP61, CmAGL24, CmNAC1*, were screened using weighted gene co-expression correlation network analysis (WGCNA) combined with correlative analysis to determine whether they play an important role in carotenoid accumulation by regulating structural genes related to the carotenoid metabolism pathway and plastid development. This study analyzed dynamic changes of carotenoid components and plastid ultrastructure of the four bud mutation cultivars of chrysanthemum and identified structural genes and transcription factors that may be involved in carotenoid accumulation. The above results laid a solid foundation for further analysis of the regulatory mechanism of the carotenoid biosynthesis pathway in chrysanthemum.

1. Introduction

Chrysanthemum × *morifolium* is a world-famous flower whose color is extremely rich. Previous studies have shown that anthocyanins and carotenoids could color the ray florets separately or together in chrysanthemum, as different proportions of anthocyanin and carotenoid accumulation determines the variation of flower color of chrysanthemum cultivars (Bai et al., 2006; Park et al., 2015). Therefore,

* Corresponding author. College of Landscape Architecture, Beijing Forestry University, Beijing, 100083, China.
** Corresponding author. College of Landscape Architecture, Beijing Forestry University, Beijing, 100083, China.
E-mail addresses: 101navy@163.com (H. Huang), silandai@sina.com (S. Dai).
[1] Contributed equally to this work.

https://doi.org/10.1016/j.plaphy.2019.07.023
Received 23 April 2019; Received in revised form 24 July 2019; Accepted 26 July 2019
Available online 02 August 2019

understanding the metabolic mechanism of these two pigments and analyzing the molecular mechanism of flower color formation will help us to directionally modify chrysanthemum color through transgenic technologies. The anthocyanin metabolic pathways of chrysanthemum have been studied in detail, and its pathway is relatively simple: two anthocyanin derivatives, Cy3-O-(6′-O-malonylglucoside) and Cy 3-O-(3′, 6′-O-dimalonylglucoside), are the main substances accumulated in ray florets (Sun et al., 2010; Park et al., 2015). All structural genes in the anthocyanin metabolic pathway and key transcription factors of the MYB-bHLH-WD40 (MBW) complex have been isolated, and their specific functions have been identified (Hong et al., 2015; Xiang et al., 2015). Compared with research on anthocyanins, the biosynthetic mechanism of carotenoids has been less studied in chrysanthemum. Thirteen structural genes related to carotenoid biosynthesis and one related to degradation have been isolated in chrysanthemum, and inhibition of *CmCCD4a* expression in white chrysanthemum petals could cause carotenoid accumulation to form yellow florets (Kishimoto and Ohmiya, 2006; Ohmiya et al., 2006), but this does not fully explain the accumulation and coloration of carotenoids. Furthermore, upstream transcription factors, which could directly regulate structural genes, have not yet been reported in chrysanthemum.

Carotenoid biosynthesis is derived from the isoprenoid pathway, and the main enzymes involved in this biosynthetic pathway are phytoene synthase (PSY), phytoene desaturase (PDS), ζ-carotene desaturase (ZDS), and carotene isomerase (CRTISO). These enzymes mainly synthesize the linear carotenes, such as phytoene, phytofluene, Z-carotene and lycopene. Lycopene is then cyclized by lycopene β-cyclase (LCYB) and lycopene ε-cyclase (LCYE) to produce α- or β-carotene, which forms carotenoids such as lutein, zeaxanthin, violaxanthin and neoxanthin under catalysis of carboxylation and cyclooxygenase such as β-carotene hydroxylase (CHYB), cytochrome P450-type carotenoid β-hydroxylase (CYP97A); cytochrome P450-type carotenoid ε-hydroxylase (CYP97C), violaxanthin de-epoxidase (VDE) and zeaxanthin epoxidase (ZEP) (Nisar et al., 2015). Carotenoid cleavage dioxygenases (CCDs) are key enzymes involved in carotenoid oxidative cleavage to decompose carotenoid polyene chain-specific double bonds to form apocarotenoids. CCDs can catalyze the degradation of carotenoids into volatile substances, abscisic acid and strigolactone (Bruno et al., 2014).Since the synthesis and storage of carotenoids mainly occur in plastids, plastid development and differentiation largely affect carotenoid accumulation. Mutations of the plastid differentiation related gene *Or* led to the accumulation of β-carotene in orange color cauliflower, indicating that this plastid differentiation gene may regulate carotenoid biosynthesis (Li and Yuan, 2013; Lu et al., 2006). In addition to the *Or* gene, plastid-lipid associated protein (PAP) also affected carotenoid accumulation by mediating plastid differentiation (Fu et al., 2012; Zeng et al., 2015; Kilambi et al., 2017). Over-expressing *PAP* in sweet pepper or tobacco significantly changed the ultrastructure of chromoplasts in leaves and petals, especially the number and distribution of plastoglobules (Rey et al., 2000). In addition, over-expression of this gene in tomato fruit increased the lycopene content and affected the ultrastructure of plastids (Simkin et al., 2007). Comparative plastid proteomics have been used to analyze the tomato stay green wild species (*Solanum habrochaites*, of which the fruit could not change color) and its cultivars and found that in addition to CHRC protein, the PAP3 protein contents in the cultivars was also significantly higher than in *S. habrochaites* (Kilambi et al., 2017).

Carotenoid regulation mainly occurs at the transcriptional level through transcription factors. Currently, transcription factors isolated and identified from model plants and crops are mainly members of the MYB, bHLH, MADS-box, NAC, and AP2/ERF families. For example, the transcription factor *CrMYB68* affected carotenoid conversion by directly inhibiting *CrBCH2* and *CrNCED5* gene expression in citrus (Zhu et al., 2017). The bHLH family transcription factor PIF1 (phytochrome interacting factor 1) identified from *Arabidopsis thaliana* interacted with the G-box on the *PSY* promoter to block its expression (Toledo-Ortiz et al., 2010). RIN (ripening inhibitor) was a member of the MADS-box transcription factor family (Vrebalov et al., 2002), which regulated carotenoid metabolism by binding to promoters of genes involved in ethylene synthesis, ethylene induction, cell wall metabolism, and carotenoid accumulation (Martel et al., 2011). In tomato, NAC4 positively regulated fruit development and carotenoid accumulation by interacting with MADS-box transcription factors RIN and NOR. The expression level of *PSY* was significantly reduced in *NAC4*-RNAi tomato lines, resulting in a 30% reduction of the total carotenoid contents, while the expression of *LCYB* and *LCYE* genes in the same line increased and were accompanied with a change in carotenoid composition (Zhu et al., 2013). However, it is unclear whether the functions of these carotenoid metabolic transcription factors are equally conserved among different species.

Bud mutants are significantly important materials for studying flower color metabolism, and the discovery of many important genes and regulatory mechanisms depends on stable mutant materials. For example, the anthocyanin regulatory gene *Pr* and the plastid development gene *Or* were isolated from purple and yellow cauliflower mutants (Chiu et al., 2010; Lu et al., 2006). Using the green skin mutant of red-skinned pear as materials, Wang et al., (2013) discovered the methylation mechanism of MYB transcription factors related to the anthocyanin biosynthesis pathway. Selection of the bud sport is the most important method for new cultivars breeding of chrysanthemum. During the long-term work of traditional Chinese chrysanthemum resource conservation, we had accumulated a set of flower color bud mutational cultivars. The original cultivar was ‘Jianliuxiang Pink’ with pink ray florets, it mutated to ‘Jianliuxiang White’, ‘Jianliuxiang Yellow’ and ‘Jianliuxiang Red’ during the planting process (Fig. 1), which were precious germplasm resources for the research of both anthocyanin and carotenoid biosynthesis.

In the present study, the carotenoid composition, content and cellular ultrastructure of the four mutation cultivars were compared to

Fig. 1. The four different color chrysanthemum cultivars (JlxW, JlxP, JlxY and JlxR).

Fig. 2. The five different developmental stages (S1–S5) of the JlxY capitulum. Bar, 1 cm.

investigate the physiological and cellular mechanisms of carotenoids involved in chrysanthemum coloration. Meanwhile, RNA sequencing (RNA-seq) libraries were constructed with outer whorls of ray florets at the S3 stage of all four cultivars and five developmental levels (S1–S5) of ray florets in 'Jianliuxiang Yellow'. Through analysis of differential gene expression and weighted gene co-expression correlation network analysis (WGCNA), we identified a group of genes that may be involved in carotenoid metabolism. Our research provided a solid foundation to analyze the regulation of carotenoid metabolism in chrysanthemum.

2. Materials and methods

2.1. Plant materials

Four flower color cultivars, 'Jianliuxiang White', 'Jianliuxiang Pink', 'Jianliuxiang Yellow', and 'Jianliuxiang Red' were used for materials. The white, pink, yellow and red cultivars were named JlxW, JlxP, JlxY and JlxR, respectively, in this study (Fig. 1). The development of chrysanthemum capitulum was divided into five stages (S1–S5) according to Sun et al., (2010) and Fig. 2. S1 was defined as when the ray florets were wrapped in bract; S2 was defined as when the ray florets had barely outgrown the bract; S3 was defined as when the ray florets completely outgrew the bract; S4 was defined as when the ray florets were fully opened; and S5 was defined as when the ray florets began to decay. The outer whorls of ray florets of these four cultivars were selected for pigmentation analysis, plastid ultrastructure observation, comparative transcriptome analysis, and WGCNA analysis.

2.2. Extraction and high-performance liquid chromatography (HPLC) analysis of carotenoids

Carotenoid components and total contents of the four cultivars were analyzed by HPLC. Briefly, 0.2 g of fresh petals of outer whorls of ray florets at S1–S5 stages were weighed into tubes then immediately frozen in liquid nitrogen. The carotenoids were released from the petals by adding 4 ml pigment extract (N-hexane: acetone: absolute ethanol = 2: 1: 1, v: v: v) and centrifuging at 6000 g for 10 min (4 °C). Then, the carotenoid extracts were dissolved by adding 2 ml methyl tert-butyl ether (MTBE) and saponified with 2 ml 10% KOH-methanol solution in the dark for 10 h. After saponification, the samples were layered by the addition of 4 ml NaCl solution (10%, w/v) and 2 ml MTBE. Supernatants (MTBE-carotenoid solution) were extracted into a new 10 ml tube, washed three times with 4 ml NaCl solution (10%, w/v), and concentrated to complete dryness using a N_2 blower. Aliquots of the extracts were redissolved in 1 ml MTBE-methanol solution (1:1, v/v) for analysis. Chromatography was performed at 25 °C with the elution program that was previously described by Park et al., (2015). Carotenoid components were identified using standards (violaxanthin, lutein, β-carotene) and published literature (Kishimoto et al. 2004, 2007; Rojas-Garbanzo et al., 2017).

2.3. Transmission electron microscopy (TEM)

In this study, we analyzed the dynamic development of plastids in outer whorls of ray florets at S1–S3 stages by TEM. Meanwhile,.TEM observation was carried out to explore the difference in plastid ultrastructure between epidermal cells and mesophyll cells in Jlx at the S3 stage of capitulum. The specific method used was described by Lado et al., (2015). Sections were stained with aqueous uranyl acetate followed by aqueous lead citrate and viewed on a Hitachi H7000 transmission electron microscope (Japan) equipped with an SIS Megaview III digital camera.

2.4. RNA-seq and data analysis of four cultivars

In this study, RNA-seq of the outer whorls of ray florets of the four cultivars at the S3 stage was performed. After extracting total RNA using a Plant RNA Rapid Extraction Kit (HUAYUEYANG Biotechnology, Beijing, China) and digesting DNA with DNase I, the mRNA was enriched with magnetic beads with Oligo (dT), and then interrupted with mRNA. Short fragments were obtained, and the first strand of cDNA was synthesized using the broken mRNA as a template. The second strand of cDNA was synthesized by the two-strand and synthesis reaction system, and the kit was used for purification and recovery and sticky end repair, and the 3′ end of cDNA was added. Next steps included base A and ligation, selection of fragment size, and finally PCR amplification. The constructed library was tested using the Agilent 2100 Bioanalyzer and the ABI StepOnePlus Real-Time PCR System. After quality testing, a cDNA fragment of approximately 200 bp length was used for double-ended sequenced on the Illumina HiseqTM 2000 sequencing platform. Connectors of the raw reads and sequences with lower quality values were removed to obtain clean reads, which were then assembled from scratch using SOAPdenovo software with the parameters set to -K29, -M2, -L50. The sequence was assembled into a contig without gaps. Finally, double-end sequencing was performed to fill the gap between different scaffolds to obtain unigene. The unigene sequences were compared with databases such as NR, Swiss-Prot, GO, KEGG, and COG and were then annotated.

2.5. Semi-quantitative reverse transcriptase-polymerase chain reaction (RT-PCR) analysis of carotenoid metabolic genes in four cultivars

To detect the expression pattern of carotenoid metabolic genes, RNA extracted from the outer whorls of ray florets in different developmental stages of the four cultivars with a plant RNA extraction kit (HUAYUEYANG Biotechnology, Beijing, China). The transcription kit synthesized cDNA as a template for RT-PCR. The specific procedure for RT-PCR was described in the methods of Zhou et al. (2008). We used *β-actin* as a reference gene to analyze the carotenoid metabolic genes including *DXS* (c106047.graph_c0), *DXR* (c124738.graph_c0), *IPI* (c107840.graph_c0), *GGPS* (c117451.graph_c0), *PSY* (c88337.graph_c0; c126482.graph_c0; c111312.graph_c0), *PDS* (c133027.graph_c1), *ZDS* (c132259.graph_c1), *CRTISO* (c131246.graph_c1), *LCYB* (c122244.graph_c0), *LCYE*

(c117576.graph_c0), *CHYB* (c74995.graph_c0), *CYP97A* (c114951.graph_c0), *CYP97C* (c129228.graph_c0), *VDE* (c128253.graph_c0), *ZEP* (c127762.graph_c2), *CCD1* (c115001.graph_c0), *CCD4a-2* (c120435.graph_c0), *CCD4b* (c115001.graph_c0), *NCED* (c126188.graph_c0). The RT-PCR primer sequences were shown in Supplementary Table 1.

2.6. RT-PCR-mediated cloning of CmCCD4a homologs

CmCCD4a, a key gene that inhibited carotenoid formation in ray florets, has been shown to consist of small gene family in chrysanthemum and this homologs usually have changed after bud sports (Yoshioka et al., 2012). For exploring whether the number of *CmCCD4a* homologs have changed after bud sports in Jlx and whether this change would affect carotenoid accumulation, isolation of *CmCCD4a* homologs in JlxW, JlxP, JlxY and JlxR was carried out in this study. The specific method used was as follow: RT-PCR was performed with ray floret cDNA of each cultivars as the template and the specific primers was used by Yoshioka et al. 2012. The PCR conditions were as follows: 94 °C for 5 min, and 35 cycles at 94 °C for 40 s, 64 °C for 30 s, and 72 °C for 90 s. PCR fragments were cloned into pGEM-T Easy Vector (Promega, America) and transformed into *Escherichia coli* DH-5α. Then using blue-white screening on X-Gal plates, 100 white individual bacterial colonies of each cultivars were selected to colony PCR using universal primer (T7, SP6), and finally 56 positive cDNA clones from JlxW, 63 from JlxP, 47 from JlxY and 50 from JlxR were obtained, then these *CmCCD4a* sequences were used for the next alignment and analysis.

2.7. Microscopic observation

In order to investigate whether the expression of *CmCCD4a-2* in the ray florets of JlxY and JlxR due to containing periclinal chimera, microscope examination of transverse sections was carried out. The specific method used was as follow: fresh ray florets of four cultivars (JlxW, JlxP, JlxY and JlxR) at the S3 stage were sliced longitudinally with paired double-edge razor blades. and placed on a slide for observation using a light microscope (Nikon Corporation, Tokyo Japan), photographs were taken using an attached camera.

2.8. Exploration of differential expression genes (DEGs) among the four cultivars

For identifying other key genes related to carotenoid accumulation in chrysanthemum, we compared transcriptome data between JlxW and JlxY, JlxW and JlxR, JlxP and JlxY, JlxP and JlxR due to the carotenoid contents between all above pairwise comparisons were significantly different. Then we took intersections from various combinations as DEGs. The DEGs were screened with a threshold false discovery rate (FDR) $< 10^{-3}$ and an absolute value of $\log_2$ ratio ≥ 1 (Wu et al., 2010). The alignment package SOAPaligner version 2.20 was used to map reads back to the transcriptome with the parameters '-m 0、-x 1000、-s 40、-l 35、-v 3、-r 2'. Then, the number of mapped clean reads for each unigene was counted and normalized into fragments per kilobase per million fragments (FPKM) values, which were widely used to calculate unigene expression (Mortazavi et al., 2008).

2.9. Homolog search and phylogenetic tree construction

For investigating the potential biological functions, phylogenetic tree of *CmPAPs* was constructed. Sequence alignments were performed using the ClustalW mode in Molecular Evolutionary Genetics Analysis version5 (MEGA5). A phylogenetic tree was subsequently constructed according to the neighbour-joining statistical method. Tree nodes were evaluated using the bootstrap method for 1000 replicates, and branches corresponding to partitions reproduced in less than 50% of the bootstrap replicates were condensed into single branches. Evolutionary distances were computed using the *p*-distance method and expressed in units of amino acid differences per site.

2.10. Transcriptome sequencing and WGCNA of ray florets of different stages in JlxY

To further analyze the regulatory mechanism of carotenoid biosynthesis and explore possible involved transcriptional factors, RNA-seq of the five developmental stages of outer whorls of ray florets in JlxY and WGCNA were performed. The sequence procedure was the same as 2.4.

For WGCNA, The R package DCGL was used to filter genes (Yang et al., 2013), leading to 29216 genes of which FPKM values > 0 were selected for further analysis. The adjacency matrix between different genes was constructed with 7 as the parameter of soft thresholding power, and the TOM similarity algorithm was used to transform the adjacency matrix into a topological overlap matrix to reduce noise and false correlation. Then, all genes were hierarchically clustered based on TO similarity. Hierarchical clustering was performed by Dynamic Hybrid Tree Cut (Zhan et al., 2015). Additionally, the expression profile of each module was summarized by representing it as the first principal component (referred to as the module eigengene), and the eigengenes of each module were correlated with the change of each carotenoid contents to find the key modules associated with carotenoid accumulation in chrysanthemum.

2.11. Real-time quantitative polymerase chain reaction (qRT-PCR) and correlation analysis

qRT-PCR was used to verify the accuracy of the transcriptome data of key genes related to carotenoid accumulation, and primer information was shown in Supplementary Table 2 qRT-PCR analysis was performed according to the SYBR Premix Ex Taq kit (Takara, Japan) with three replicates, and PCRs were performed using a Mini Opticon Real-time PCR System (Bio-Rad, USA) (Fu et al., 2014).

To further screen the key transcription factors that may be involved in the carotenoid biosynthesis pathway of chrysanthemum, we used OriginPro8.0 software to analyze the linear regression coefficient R^2 between the qRT-PCR data of key transcription factors and the total carotenoid contents. We then identified candidate transcription factors related to carotenoid accumulation according to the R^2 value.

3. Results

3.1. Carotenoid contents and composition analysis of the four chrysanthemum cultivars

Carotenoids are one of the important pigments that affect the flower color of chrysanthemum. To determine whether the different colors of these four cultivars (JlxW, JlxP, JlxY and JlxR) are due to different types of carotenoids, the carotenoid components of the outer whorls of ray florets at a later developmental stage (S4) of four chrysanthemum cultivars were identified by HPLC. We found that the carotenoid components of the four cultivars were similar, including lutein (peak 8) and its isomer (9*Z*)-lutein (peak 9), (9′*Z*)-lutein (peak 10), and lutein derivatives lutein-5,6-epoxide (peak 4) and its isomer (9′*Z*)-lutein-5,6-epoxide (peak 7), (9*Z*,9′*Z*)-lutein-5,6-epoxide (peak 5). Additionally, violaxanthin (peak 1), α-carotene (peak 11), β-carotene (peak 12), and (9*Z*)-β-carotene (peak 13) were also identified (Fig. 3; Table 1).

The dynamic changes of each carotenoid component in ray florets were analyzed by HPLC. It was found that at the early developmental stage of capitulum (S1), all four cultivars were able to accumulate carotenoids in the ray florets, and the total contents was similar (9.71–15.08 μg/g). In addition, the carotenoid components were identical, including violaxanthin, (9*Z*, 9′*Z*)-lutein-5,6-epoxide, 5,6-epoxide, (9′*Z*)-lutein-5,6-epoxide, lutein, α-carotene, β-carotene and (9*Z*)-β-carotene, among which violaxanthin, lutein and β-carotene were the most important carotenoids, accounting for 69.7%–75.1% of the total carotenoids (Fig. 4). During capitulum development, the components and total carotenoid contents in JlxW and JlxP gradually decreased, and at

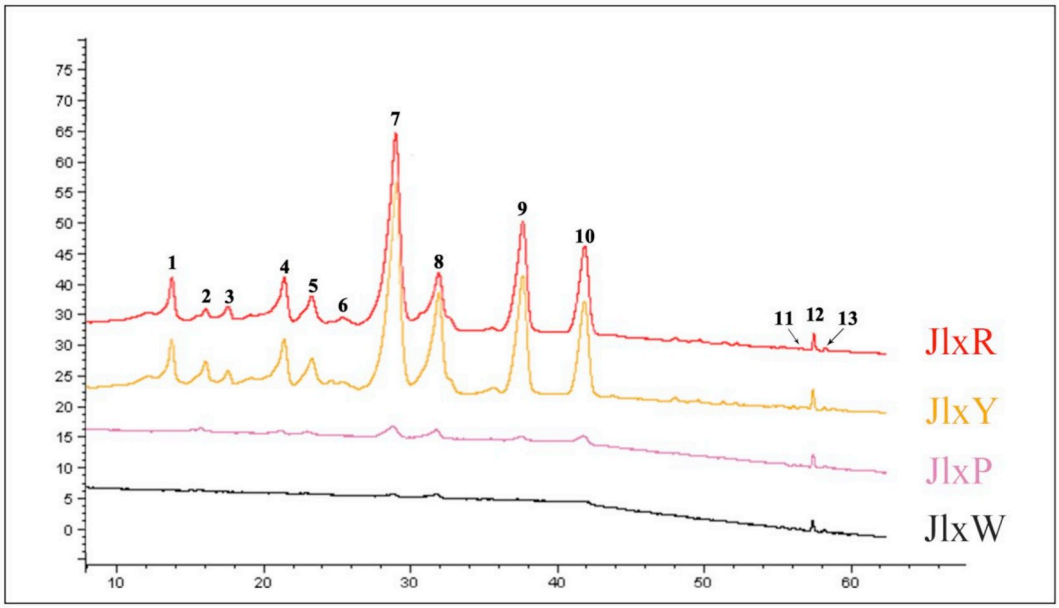

Fig. 3. High-performance liquid chromatography (HPLC) analysis (450 nm) of carotenoid components in the ray florets of JlxW, JlxP, JlxY and JlxR at the S4 stage.

the S4 stage, the total contents was 1.97 and 3.13 μg/g, respectively, which was only 13% and 25% of the contents at S1. At the S5 stage, only traces of carotenoids accumulated in JlxW (0.11 μg/g) and JlxP (0.12 μg/g). In contrast, the total carotenoid contents increased significantly in JlxY and JlxR, reaching a maximum of 97.95 and 137.35 μg/g at the S4 stage, respectively, which was 10.08- and 13.57-fold higher than the contents at the S1 stage. In addition, lutein, lutein isomer (9*Z*)-lutein, (9′*Z*)-lutein and lutein 5,6-epoxide, (9′*Z*)-lutein-5,6-epoxide and (9*Z*,9′*Z*)-lutein-5,6-epoxide were the most important carotenoid components, accounting for 89.4% and 84.2% of the total contents. As the main carotenoid component at the early developmental stage (S1), however, the content of β-carotene gradually decreased during capitulum development, only accounting for 0.17–0.34% of the total carotenoids at the S4 stage. At the S5 stage, the total carotenoid contents (82.58, 66.67 μg/g) had decreased in the ray florets of JlxY and JlxR compared with the S4 stage (Fig. 4).

3.2. Comparative ultrastructure of plastids in four cultivars

Since carotenoids are synthesized and stored in plastids, plastid development can greatly affect carotenoid metabolism. To investigate the morphological changes of plastids during capitulum development in the four cultivars, TEM was used to observe the plastid ultrastructure of the outer whorls of ray florets. The results showed that there were two different types of plastids in the ray florets of all cultivars at the early developmental stage of the capitulum (S1). One of them contained starch grains, undeveloped thylakoids, and a small amount of plastoglobules, which were regarded as undeveloped chloroplasts (Fig. 5A, C, E, G); another type of plastid contained proplastids, which contained an undifferentiated stroma (Fig. 5B, D, F, H), and were quite similar to the ultrastructures presented in the white-flesh loquat (Fu et al., 2012).

As the capitulum developed to the S2 stage, the chloroplasts of all cultivars displayed more obvious thylakoid membranes and a significant increase in the number of plastoglobules (Fig. 5I, K, M, O). However, the developmental pattern of proplastids was extremely different among the four cultivars. For JlxW and JlxP, the morphology of the proplastids did not change, and a great number of undifferentiated stroma still existed (Fig. 5J, L). The proplastids of JlxY and JlxR gradually differentiated into the ultrastructure of chromoplasts, such as plastoglobules and tubules (Fig. 5N, P), which were regarded as the typical intermediate types of transformation from proplastids to chromoplasts.

Table 1
Identification of main carotenoid components in the ray florets of JlxW, JlxP, JlxY and JlxR.

Peak number	Retention time (min)	HPLC-DAD UV/Vis spectrum (nm)				%III/II	%AB/AII	Tentative identification
		cis-peak	I	II	III			
1	13.297	–	418	440	470	91.36	–	violaxanthin
2	15.603	–	416	438	465	47.43	–	Unidentified 1
3	17.521	–	406	430	458	52.13	–	Unidentified 2
4	20.914	–	416	440	468	83.25	–	lutein-5,6-epoxide
5	23.711	329	416	441	467	83.32	10.36	(9*Z*,9′*Z*)-lutein-5,6-epoxide
6	25.179	–	410	432	460	84.38	–	Unidentified 3
7	28.473	328	413	435	463	84.23	9.27	(9′*Z*)-lutein-5,6-epoxide
8	32.051	–	425	444	472	66.21	–	lutein
9	37.122	332	416	440	468	57.13	7.17	(9*Z*)-lutein
10	42.531	328	417	442	468	56.19	8.26	(9′*Z*)-lutein
11	55.224	–	422	444	474	52.69	–	α-carotene
12	57.711	–	421	452	480	32.27	–	β-carotene
13	58.632	340	422	448	471	33.13	8.38	(9*Z*)-β-carotene

% III/II is the ratio of the peak height of band III to that of band II.
% AB/AII is the ratio of the height of the *cis*-peak band to that of band II.

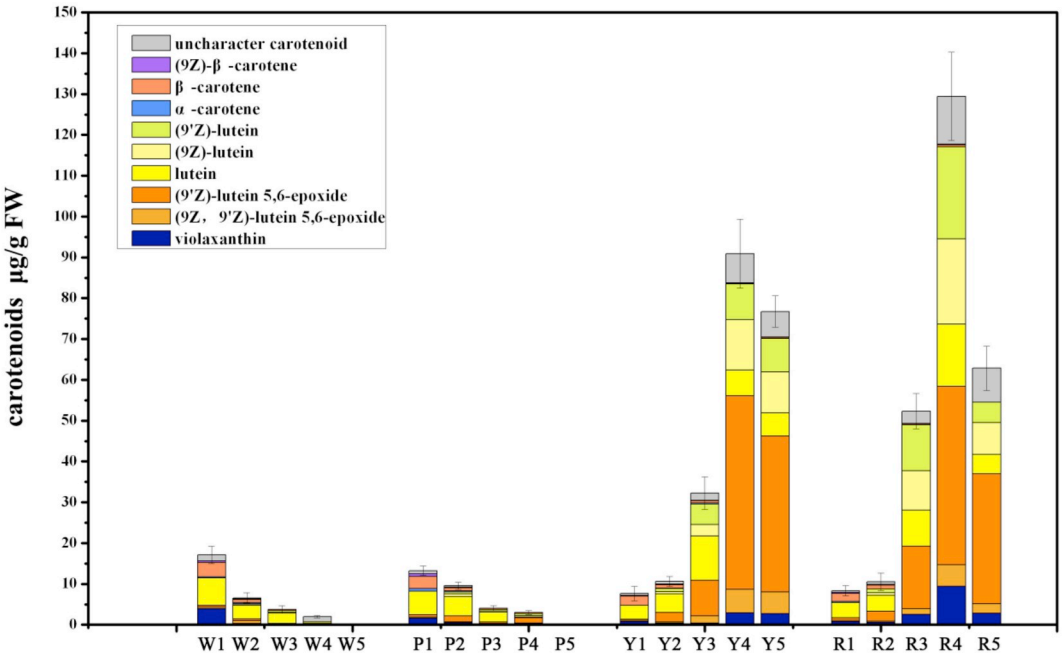

Fig. 4. Changes of carotenoid compositions and contents in the four chrysanthemum cultivars at the five developmental stages. W1–W5, P1–P5, Y1–Y5, and R1-R5 are representing five developmental stages (S1–S5) of the capitulum of JlxW, JlxY, JlxP and JlxR respectively. Data of carotenoids are mean ± SE of three replicates.

At the S3 stage, there were still two plastid types in JlxW and JlxP: one type derived from the degraded chloroplasts, which was characterized by a loose structure, broken membrane system, and overflowing plastoglobules (Fig. 5R, T), and the other type was still proplastid. Compared with the S1 and S2 stages, a large number of lipid vesicles appeared, while undifferentiated stroma still existed (Fig. 5Q, S). The chloroplasts and protoplasts in the ray florets of JlxY and JlxR were completely transformed into chromoplasts, and the chromoplasts of JlxY only contained plastoglobules (Fig. 5U, V), while the chromoplasts of JlxR contained both plastoglobules and tubules, which were regarded as tubular-globular chromoplasts (Fig. 5W, X).

3.3. Transcriptome sequencing, de novo assembly, functional annotation and classification

RNA-seq of the four cultivars was performed to explore the molecular mechanism of carotenoid accumulation in chrysanthemum. A total of 86,438 unigenes were assembled, with the size of 69,420,297 bp and N50 of 1186 bp, and 22,250 of the annotated unigenes were longer than 1000 bp. A total of 86,438 unigenes were annotated based on BLASTx (E-value $< 1 \times 10^{-5}$) searches against the following public databases: Nr, COG, Pfam, KOG, Swiss-Prot, KEGG and GO. Among them, 46,727 (54.06%) unigenes could be annotated to the Nr protein database, 34,883 (40.35%) unigenes could be annotated to the Pfam database and 32,632 (37.75%) unigenes could be annotated to the Swiss-Prot protein database. We used GO, COG, and KEGG assignments to classify the functions of the predicted unigenes. A total of 28,813 (33.33%) unigenes were categorized into 55 GO functional groups distributed under three main categories: biological processes, cellular components and molecular functions. Under the biological processes category, proteins related to “oxidation-reduction process (GO:0055114)”, “translation (GO:0006412)” and “protein phosphorylation (GO:0006468)” were the most enriched items. Proteins related to “plasma membrane (GO:0005886)”, “integral component of membrane (GO:0016021)” and “nucleus (GO:0005634)” were enriched in the cellular components category. In the molecular functions category, “ATP binding (GO:0005524)”, “metal ion binding (GO:0046872)” and “zinc ion binding (GO:0008270)” were the most highly represented GO terms. Furthermore, 16,457 (19.03%) unigenes were categorized into COG functional groups with 25 categories. In addition to COG analysis, KEGG pathway mapping could indicate the possible biological interpretation of the assigned functions. A total of 20,076 (23.22%) unigenes were mapped into KEGG pathways. The most represented pathways were “Ribosome (ko03010)”, “Carbon metabolism (ko01200)” and “Biosynthesis of amino acids (ko01230)”.

3.4. Expression analysis of carotenoid metabolic genes in four cultivars

By comparing the carotenoid contents and composition between these four cultivars, we found that the main pigments in chrysanthemum were lutein, lutein isomer and their derivatives. Furthermore, the total carotenoid contents accumulated in JlxY and JlxR (97.95 and 137.35 μg/g respectively) was much higher than that of JlxW and JlxP (1.97 and 3.13 μg/g, respectively) (Fig. 4). To investigate if these significant differences in carotenoid accumulation among the four cultivars were caused by the expression of carotenoid metabolic genes, structural genes related to carotenoid biosynthesis pathways in the transcriptome database were fully exploited, including genes related to synthetic pathway: *DXS* (c106047.graph_c0), *DXR* (c124738.graph_c0), *IPI* (c107840.graph_c0), *GGPS* (c117451.graph_c0), *PSY* (c88337.graph_c0, c126482.graph_c0, c111312.graph_c0), *PDS* (c133027.graph_c1), *ZDS* (c132259.graph_c1), *CRTISO* (c131246.graph_c1), *LCYB* (c122244.graph_c0), *LCYE* (c117576.graph_c0), *CHYB* (c74995.graph_c0), *CYP97A* (c114951.graph_c0), *CYP97C* (c129228.graph_c0), *VDE* (c128253.graph_c0), *ZEP* (c127762.graph_c2); genes related to carotenoid degradation: *CCD1* (c115001.graph_c0), *CCD4a-2* (c120435.graph_c0), *CCD4b* (c115001.graph_c0), *NCED* (c126188.graph_c0), etc. The fragments per kilobase of exon per million reads mapped (FPKM) of carotenoid metabolic genes in the transcriptome showed that the average expression levels of *CmLCYE* in JlxY and JlxR were 2.04-fold higher than those in JlxW and JlxP, while the average expression level of *CmCCD4a-2* related to carotenoid degradation in JlxY and JlxR was only 34.75% of the expression level in JlxW and JlxP. The other genes showed similar expression patterns in the four cultivars (Fig. 6), and the results of RT-PCR were consistent with the transcriptome data (Fig. S1). The above results indicated that *CmLCYE* and *CmCCD4a-2* likely affected carotenoid accumulation in chrysanthemum.

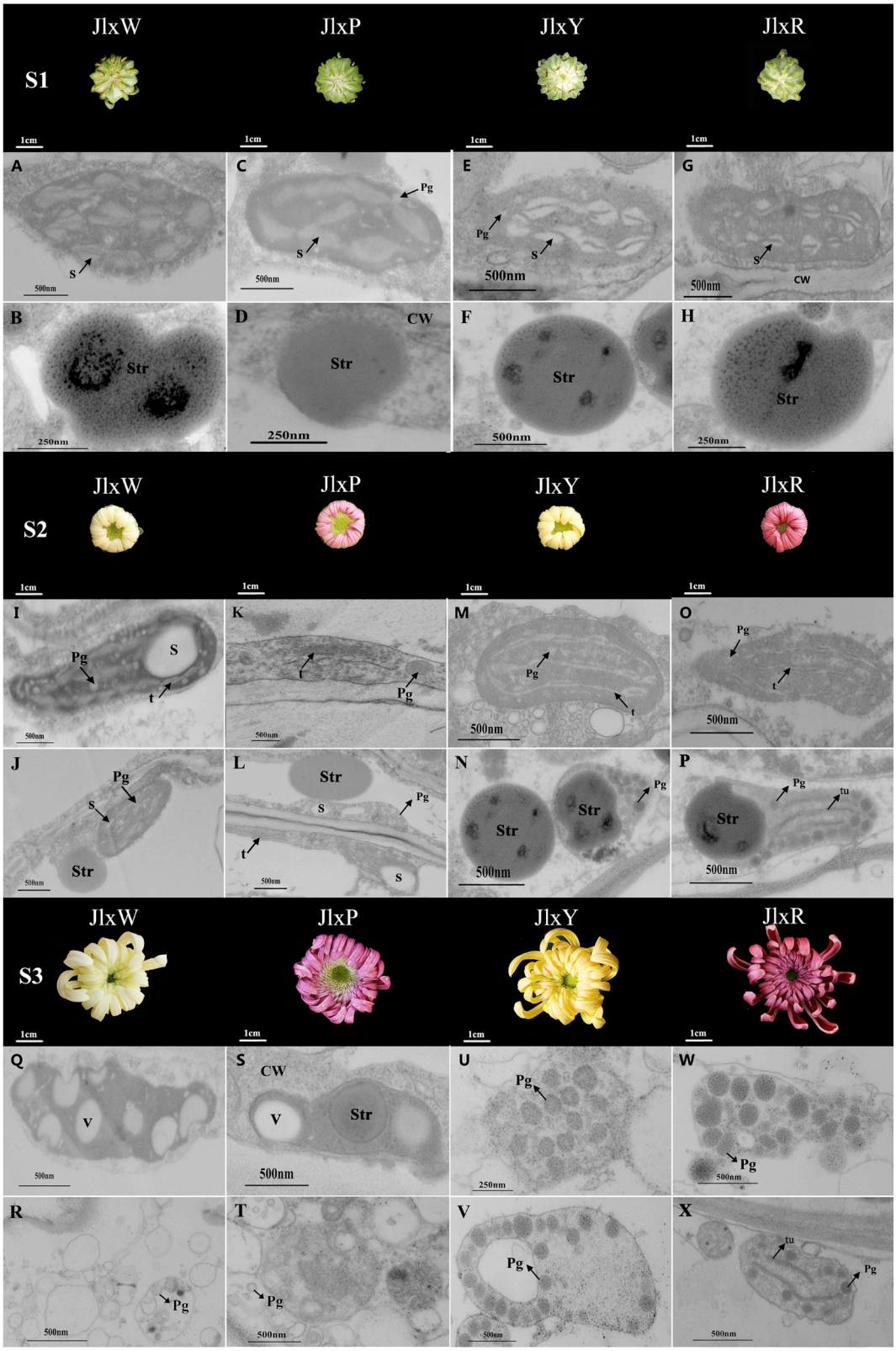

Fig. 5. TEM observation of the plastids in the four chrysanthemum cultivars at the S1–S3 stages of capitulum. A-H. Plastid ultrastructure in the ray florets of JlxW, JlxP, JlxY and JlxR cultivars at the S1 stage. I–P. Plastid ultrastructure in the ray florets of JlxW, JlxP, JlxY and JlxR cultivars at the S2 stage. Q-X. Plastid ultrastructure in the ray florets of JlxW, JlxP, JlxY and JlxR cultivars at the S3 stage. S: starch grains; T: thylakoids; Pg: plastoglobule; V: lipid vesicles; Str: undifferentiated stroma; Tu: tubules; CW: cell wall.

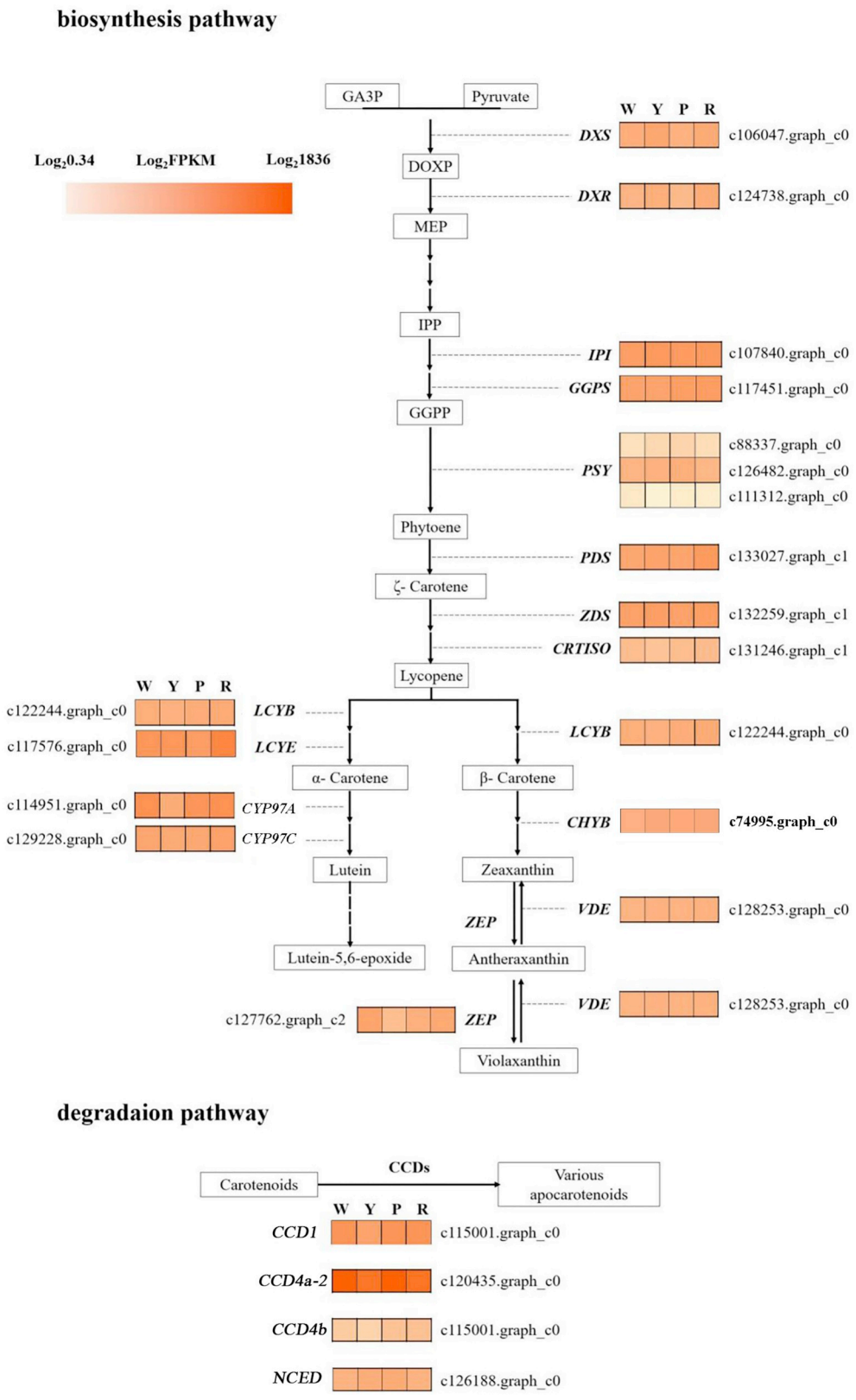

Fig. 6. Expression of the structural genes of the carotenoid metabolic pathway in JlxW (W), JlxP (P), JlxY (Y) and JlxR (R) cultivars at the S3 stage according to transcriptome database. The genes involved in carotenoid metabolism including *DXS:* 1-deoxy-D-xylulose-5-phosphate-synthase; *DXR:* DXP reductoisomerase; *IPI:* isopentenyl pyrophosphate isomerase; *GGPS:* geranylgeranyl diphosphate synthase; *PSY1:* phytoene synthase; *PDS:* phytoene desaturase; *ZDS:* ζ-carotene desaturase; *CRTISO:* carotene isomerase; *LCYB:* lycopene β-cyclase; *LCYE:* lycopene ε-cyclase; *CHYB:* β-carotene hydroxylase; *CYP97A:* cytochrome P450-type carotenoid β-hydroxylase; *CYP97C:* cytochrome P450-type carotenoid ε-hydroxylase; *VDE:* violaxanthin de-epoxidase; *ZEP:* zeaxanthin epoxidase; The metabolites involved in carotenoid biosynthesis pathway including GA3P: D-glyceraldehyde 3-phosphate; Pyruvate: DOXP, 1-deoxy-D-xylulose 5-phosphate; MEP: 2-C-methyl-D-erythritol 4-phosphate; IPP: isopentenyl pyrophosphate; GGPP: geranylgeranyl diphosphate; The genes involved in degration pathway includin *CCD:* carotenoid cleavage dioxygenase; *NCED*: 9-*cis*-epoxycarotenoid dioxygenase.

3.5. Cloning of CmCCD4a homologs

CmCCD4a, a single dominant gene that inhibited carotenoid formation or accumulation in ray florets, has been shown to consist of small gene family (*CmCCD4a-1* to *6*) in chrysanthemum, and this homologs usually have changed after bud sports (Yoshioka et al., 2012; Ohmiya et al., 2012). In this study, we would explore whether the number of *CmCCD4a* homologs have changed after bud sports in Jlx and whether this change would affect carotenoid accumulation. By RT-PCR mediated cloning, blue-white screening on X-Gal plates and colony PCR detection, we obtained 56 *CmCCD4a* positive cDNA clones from JlxW, 63 from JlxP, 47 from JlxY and 50 from JlxR respectively, The

nucleotide sequences of all obtained positive clones was completely identical with *CmCCD4a-2* (Yoshioka et al., 2012), while *CmCCD4a-1, -3, -4, -5, -6* were not detected (Supplementary Table 3), it was shown that *CmCCD4a-2* was the main homolog expressed in JlxW, JlxP, JlxY and JlxR. Similarly, *CmCCD4a-2* was also the main transcripts in chrysanthemum cultivar '94–765' (Yoshioka et al., 2012). In a word, We found that *CCD4a* homolog had not changed in Jlx.

3.6. Light microscope and TEM observation of transverse sections of ray florets

Cultivars derived from bud sports generally have chimerical structure, Ohmiya et al., (2006) and Yoshioka et al., (2012) have found that some yellow-flowered chrysanthemum cultivars which expressed *CmCCD4a* in ray florets usually existed periclinal chimera, and either the L1 or the L2 layer may behave genetically in a manner identical to that of the white chrysanthemum cultivars. In this study, microscope examination of transverse sections of ray florets was carried out for investigating whether the expression of *CmCCD4a-2* in the ray florets of JlxY and JlxR due to containing periclinal chimera. We found that in the sections of JlxW and JlxP, there was no yellow pigmentation in the ray florets, and TEM observation showed that there were no chromoplast existed in adaxial epidermis (L1 layer) or mesophyll (L2 layer). While in the sections of JlxY and JlxR, yellow pigmentation was localized in the adaxial epidermis due to exsiting globular chromoplasts (L1 layer), and the underlying mesophyll (L2 layer) appeared to be white owing to just contain proplastids with lipid vesicles (Fig. S2; Fig. S3). It showed that *CmCCD4a-2* could express in the ray florets of JlxY and JlxR due to their chimerical structure.

3.7. Screening for carotenoid-related DEGs by comparative transcriptome analysis

For identifying other key genes related to carotenoid accumulation in chrysanthemum, the transcriptome data of the four cultivars was compared. Multiple comparisons between the four cultivars showed that in total, 302 DEGs were predicted to be involved in carotenoid accumulation in chrysanthemum (Fig. 7, Supplementary Table 4). Among the 302 DEGs, *CmLCYE* (c117576.graph_c0) and *CmCCD4a-2* (c50217.graph_c0) were the key factors reported to affect carotenoid accumulation in chrysanthemum. We also found that among the 302 DEGs, genes involved in plastid differentiation and development, such as *PAP* genes (*Pg-1*, c127662.graph_c0; *PAP10*, c128060.graph_c0; *PAP13*, c118892.graph_c0, Fig. S4) related to chromoplast differentiation and plastoglobule formation, expressed distinctly higher in JlxY and JlxR than in JlxW and JlxP. These results were in accordance with the ultrastructural analysis results that proplastids and chloroplasts in the ray florets of JlxY and JlxR can transform into chromoplasts, while that would not occur in JlxW and JlxP (Fig. 5). Moreover, the expression levels of ethylene synthesis related gene *ACO* (1-aminocyclopropane-1-carboxylate oxidase homolog 1-like, c96394.graph_c0) in JlxW and JlxP with trace carotenoids was much higher than that in JlxY and JlxR. Ethylene often affected carotenoid accumulation by regulating plant development (Su et al., 2015; Wisutiamonkul et al., 2017), and *ACO* may be regarded as a negative regulator in carotenoid metabolism in chrysanthemum. The results of qRT-PCR supported the reliability of the comparative transcriptome analysis described above (Fig. 8).

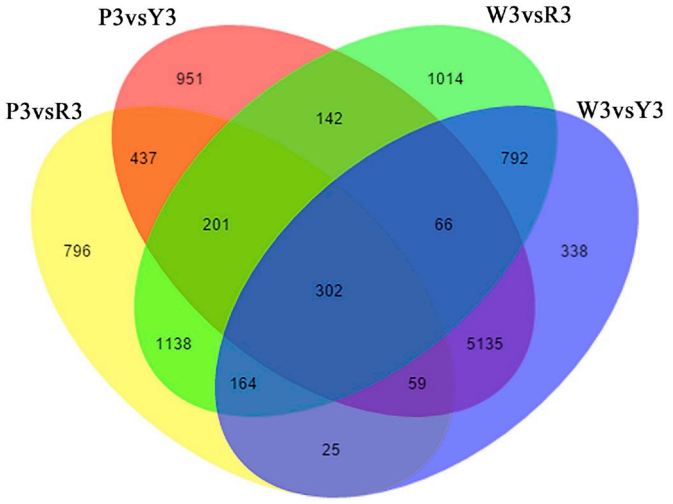

Fig. 7. Venn diagram of differentially expressed genes (DEGs) between four color cultivars. 'W3' vs 'Y3', 'W3' vs 'R3', 'Y3' vs 'P3', 'P3' vs 'R3' are representing the DEGs between the JlxW and JlxY, JlxW and JlxR, JlxY and JlxP, JlxP and JlxR at the S3 stage of capitulum, respectively.

3.8. Screening for transcription factors regulating carotenoid accumulation through WGCNA

The expression of structural genes involved in carotenoid metabolism and plastid development in higher plants is often directly regulated by upstream transcription factors. In this study, we used five developmental stages (S1–S5, Fig. 2) of ray florets of JlxY as materials to build transcriptome libraries and explored the potential transcription factors that regulated carotenoid accumulation in chrysanthemum using WGCNA combined with the analysis of dynamic changes of carotenoid composition and total contents in five different developmental stages. First, the expression patterns of 29,216 DEGs obtained from transcriptome sequencing were analyzed by WGCNA, and they were divided into 50 modules according to the similarity of expression patterns (Fig. 9A). The eigengenes of each module represent the gene expression profile of the entire module, and a total of 50 different expression patterns were obtained (Fig. S5). Because the pattern of gene expression was often associated with phenotypic changes, such as pigment accumulation and organ development in higher plants (Feng et al., 2017; Yang et al., 2018), we analyzed the correlation between the expression patterns of each module and the changes of the total contents and carotenoid components, which included violaxanthin, (9*Z*,9′*Z*)-lutein-5,6-epoxide, (9′*Z*)-lutein-5,6-epoxide, lutein, (9*Z*)-lutein, (9′*Z*)-lutein, α-carotene, β-carotene, (9*Z*)-β-carotene. The results showed that the pierson correlation coefficient of the module 'darkturquoise' with the main carotenoid components, such as (9*Z*)-lutein, (9′*Z*)-lutein, (9′*Z*)-lutein-5,6-epoxide and total carotenoid contents was the highest, which were 0.99, 0.89, 0.99, and 0.98, respectively (Fig. 9B), indicating that the module 'darkturquoise' was closely related to carotenoid accumulation in chrysanthemum.

Deep analysis revealed that the 'darkturquoise' module contained a total of 1493 genes, including *CCD* (TRINITY_DN71578_c3_g1) involved in carotenoid degradation and *PAPs* involved in plastoglobule formation (TRINITY_DN58718_c0_g1; TRINITY_DN64501_c0_g2). This finding further indicated that carotenoid degradation and plastid development genes were essential for the accumulation of chrysanthemum carotenoids. In addition to the genes mentioned above, there were 42 regulatory transcription factors found in module darkturquoise, belonging to WRKY, bHLH, MYB, ARF/AUX-IAA, NAC, ERF, bZIP, HSF, MADS-BOX, Zinc finger protein, DREB, and Nuclear Y transcription factor families (Supplementary Table 5).

To find key genes from the module 'darkturquoise', we constructed a gene correlation network using 1493 genes in this module. Based on the degree of connectivity, the top 100 genes were regarded as Hub genes. Of the 100 Hub genes, 12 transcription factors were found, including CmMYB305 (TRINITY_DN48859_c0_g1), CmMYB1 (TRINITY_DN63887_c1_g1) and CmRAD3 (RINITY_DN60137_c0_g2) belonging to the MYB transcription factor family; CmbHLH62 (TRINITY_DN58707_c0_g1), CmUNE10 (TRINITY_DN63420_c0_g1), and CmbHLH148 (TRINITY_DN61484_c0_g1) belonging to the bHLH transcription factor family; CmWRKY57 (TRINITY_DN57783_c5_g2) and CmWRKY25 (TRINITY_DN52772_c0_g1) belonging to the WRKY transcription factor family; the

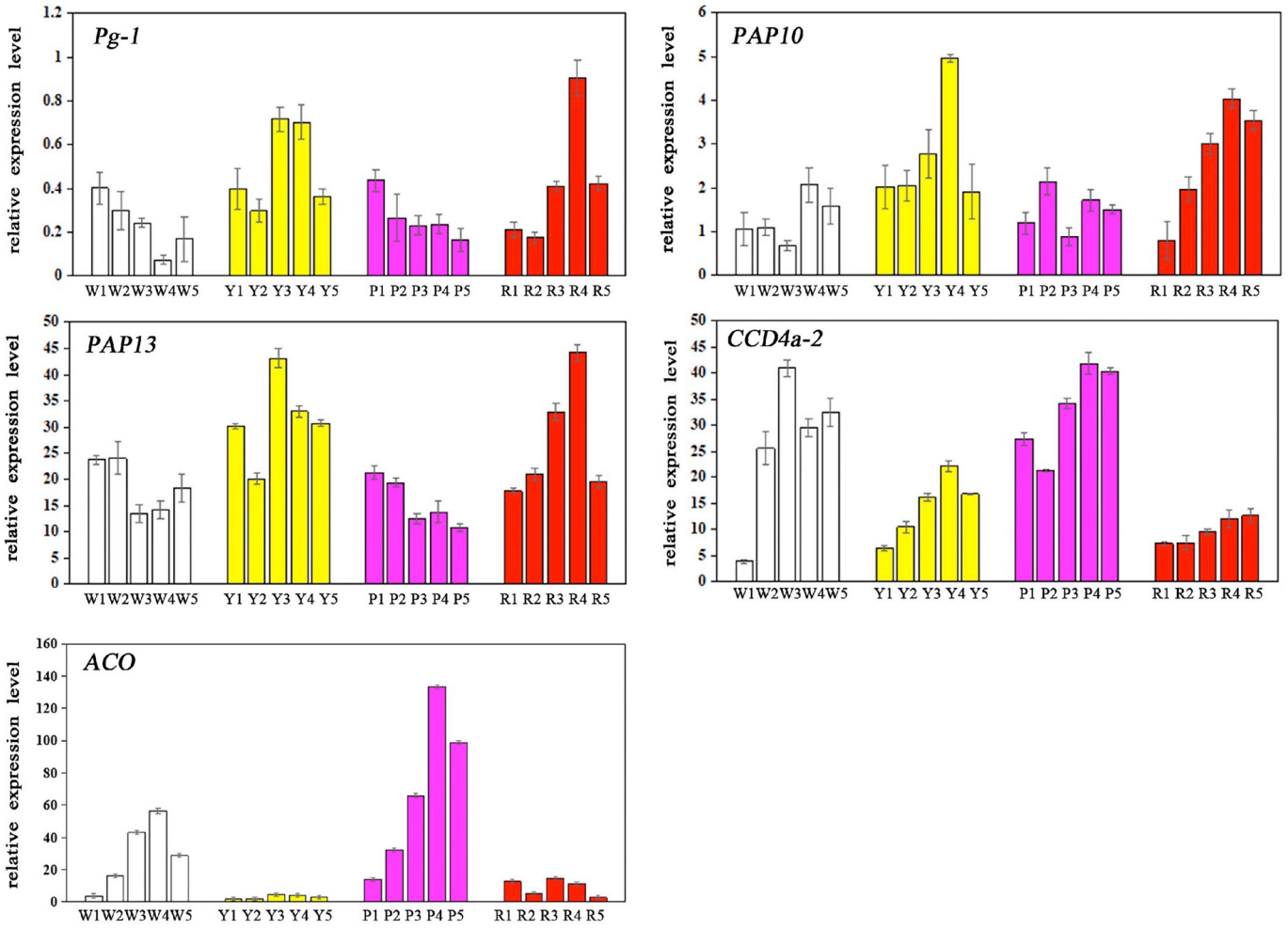

Fig. 8. Expression analysis of DEGs byqRT-PCR. W1–W5, P1–P5, Y1–Y5, and R1-R5 are representing five developmental stages (S1–S5) of the capitulum of JlxW, JlxY, JlxP and JlxR respectively.

CmTGA1 (TRINITY_DN55627_c1_g1) and CmbZIP61 (TRINITY_DN52523_c0_g1) belonging to the bZIP transcription factor family; CmNAC1 (TRINITY_DN58894_c0_g1) belonging to the NAC transcription factor family; and CmARF19 (TRINITY_DN56086_c1_g6) belonging to the ARF transcription factor family (Fig. S6).

The gene expression patterns of these 12 transcription factors were analyzed by qRT-PCR and correlated with the changes of total carotenoid contents. The results showed that 6 of these transcription factors were significantly correlated with the dynamic changes of carotenoids ($R^2 > 0.9$), including CmMYB305 (TRINITY_DN48859_c0_g1, $R^2 = 0.9609$), CmMYB29 (TRINITY_DN59637_c3_g2, $R^2 = 0.9075$), CmRAD3 (TRINITY_DN60137_c0_g2, $R^2 = 0.9124$), CmbZIP61 (TRINITY_DN52523_c0_g1, $R^2 = 0.9576$), CmAGL24 (TRINITY_DN62353_c3_g1, $R^2 = 0.9719$), and CmNAC1 (TRINITY_DN58894_c0_g1, $R^2 = 0.9717$) (Fig. 10). Among of them, transcription factor *CmNAC1,* which was located at the center of the gene expression regulatory network, expressed higher in JlxY and JlxR than JlxW and JlxP (Fig. S7). These results suggested that these transcription factors, especially in *CmNAC1*, might be involved in the metabolic regulation of carotenoids in chrysanthemum.

4. Discussion

4.1. LCYE and CCD4a-2 determine the carotenoid metabolic pathway in chrysanthemum

Bud mutants are significantly important materials for analysis of the regulation of carotenoid metabolism. In this study, we found that ray florets of the four bud mutation cultivars could accumulate carotenoids at the early developmental stage of the capitulum (S1), and its contents and components were similar, mainly including violaxanthin, lutein and β-carotene. These chloroplast-type carotenoids was consistent with fruits such as loquat, citrus, and tomato (Fu et al., 2012; Kato et al., 2004; Kilambi et al., 2017) and petals such as Japanese morning glory, eustoma and carnation at the early developmental stage (Yamamizo et al., 2009; Liu et al., 2013; Ohmiya et al., 2013). As the capitulum developed, each component and total carotenoid contents were significantly reduced, and only trace carotenoids existed in JlxW and JlxP. However, carotenoid contents increased significantly in JlxY and JlxR at the S4 stage, and the total contents was found to be 10.08 and 13.57 times greater than that in the early stage (S1). Lutein, lutein isomers and lutein derivatives belonging to the α-branch were the most important carotenoid components, accounting for 89.4%, 84.2% of total carotenoid contents in JlxY and JlxR, respectively. *LCYE* was a key gene controlling carotenoid metabolism whose high expression often caused the carotenoid metabolic pathway to be dominated by the α-branch (Pogson and Rissler, 2000). For example, the expression of *LCYE* in *Osmanthus frangrans* cultivar 'Jingui' was significantly higher than in other color cultivars, leading to accumulation of large amounts of α-branch lutein (Han et al., 2014). In this study, we found that the expression of *LCYE* in JlxY and JlxR was higher than in JlxW and JlxP. Meanwhile, the ratio of *LCYE* expression to *LCYB* increased from 2.33 to 6.07 with capitulum development. Therefore, it was speculated that the high expression of *LCYE* may be the reason the accumulation of

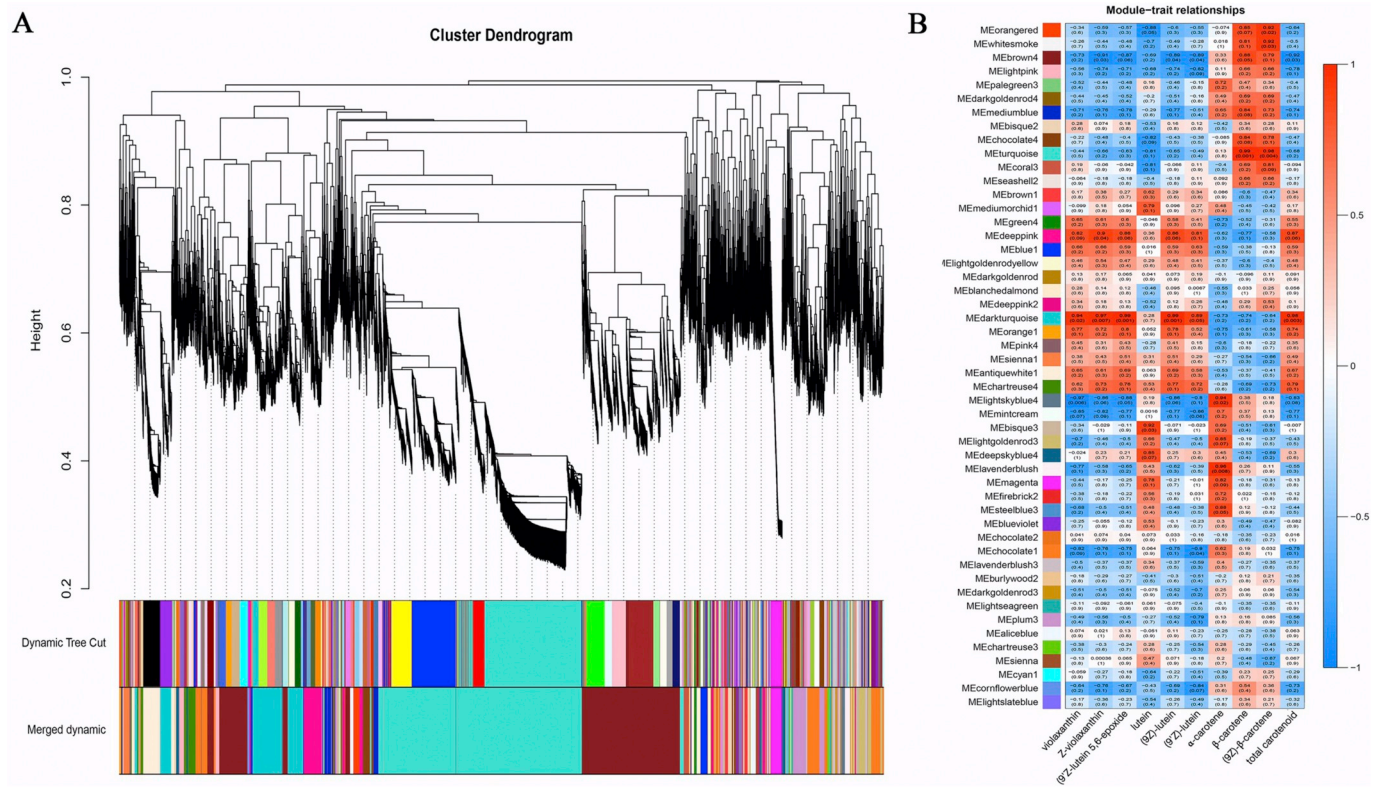

Fig. 9. Network analysis dendrogram showing modules identified by weighted gene co-expression network analysis (WGCNA). A. Dendrogram plot with color annotation. B. Module-carotenoid weight correlations and corresponding *P*-values. The left panel shows the 50 modules. The color scale on the right shows module-trait correlation from −1 (blue) to 1 (red). (For interpretation of the references to color in this figure legend, the reader is referred to the Web version of this article.)

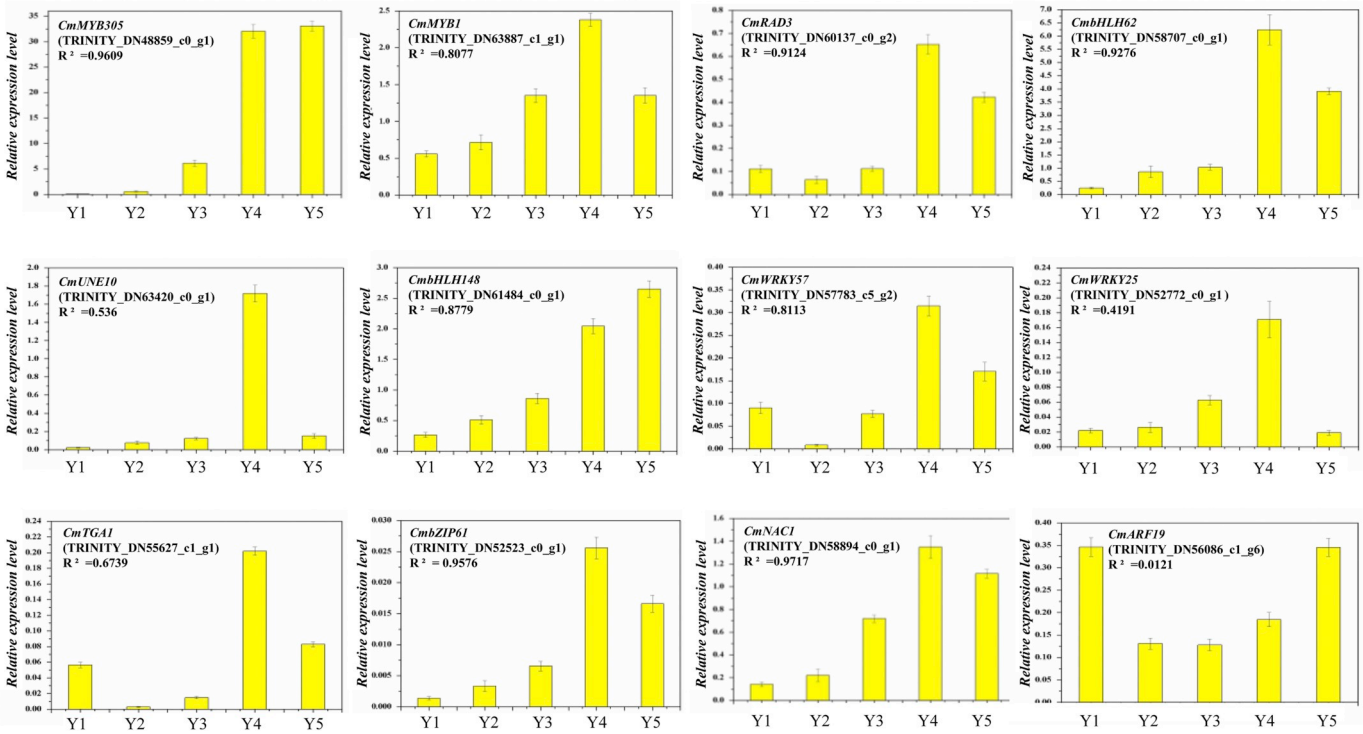

Fig. 10. Relative expression levels of twelve transcription factors related to carotenoid biosynthesis by qRT-PCR. The x-axis and y-axis represent the five developmental stages of the JlxY's capitulum and the relative expression level of each gene, respectively. R^2 represents correlation analysis between relative expression levels of genes and the accumulation of carotenoid contents.

lutein and its derivatives in the ray florets of chrysanthemum. And *CmCCD4a-2*, which was involved in carotenoid degradation (Ohmiya et al., 2006; Yoshioka et al., 2012), was the key factor that determining carotenoid accumulation in chrysanthemum. In this study, *CmCCD4a-2* could express higher in JlxW and JlxP than JlxY and JlxR, and its transcriptional level was also significantly higher than other carotenoid metabolic genes (Fig. 6). Meanwhile, due to existing chimerical structure in JlxY and JlxR, which was consistent with previous studies (Ohmiya et al., 2006; Yoshioka et al., 2012), *CmCCD4a-2* only expressed in the L2 layer of ray florets to degrade carotenoids but not in the L1 layer. Thus, the L1 layer of JlxY and JlxR's ray florets could accumulate carotenoids and appear to be yellow. Furthermore, we also found the other key genes that were not involved in the carotenoid metabolic pathway could affect carotenoid accumulation in chrysanthemum.

4.2. Chromoplast transformation and PAPs influence the carotenoid accumulation in chrysanthemum

As plastids are the main organelles that synthesize and store carotenoids, carotenoid accumulation is largely influenced by plastid development and differentiation. Chromoplasts are the “sinks” that lead to carotenoid coloration and its differentiation plays an important role in the regulation of carotenoid accumulation and final coloration (Li and Yuan, 2013; Lu and Li, 2008; Nazia et al., 2015). Kim et al., (2010) found that white carrots did not accumulate carotenoids due to the small number of chromoplasts compared to other cultivars. Similarly, as carotenoids were in crystalline form in the chromoplasts of red-fleshed loquat cultivar while no chromoplasts were found in the cells of the fully ripening white-fleshed cultivar, the carotenoid contents in the red-fleshed cultivar was approximately 40 times higher than that of the white-fleshed cultivar (Fu et al., 2012). In this study, chloroplasts and proplastids were found in the ray florets at the S1 stage of four cultivars. With the development of the capitulum, the chloroplasts had degraded, and the proplastids formed a number of lipid vesicles in JlxW and JlxP. However, for JlxY and JlxR, the chloroplasts and proplastids in the ray florets were completely transformed to chromoplasts, which produced ultrastructures such as plastid globules and tubules (Fig. 4). In conclusion, we speculated that the abnormal differentiation of chromoplasts may be an important reason for the differential accumulation of carotenoids in these four cultivars.

Chromoplast differentiation of higher plants could be observed using light microscopy and TEM, and it was not until 2006 that the gene controlling chromoplast formation was discovered, namely, the *Or* gene of cauliflower, which can control the transformation from protoplasts into chromoplasts in yellow cauliflower mutants (Lu et al., 2006). In addition, a large number of studies have shown that *PAP* can affect the differentiation of chromoplasts and carotenoid accumulation. Pan et al., (2012) found that the abundance of *PAP* expression increased in the red-flesh orange ‘Hong Anliu’ during fruit maturation. Plastid proteomics also showed that the contents of CitPAP1 and CitPAP4 protein increased significantly with the conversion of amyloplasts into chromoplasts in sweet orange, and these proteins accounted for 68.5% of the total chromoplasts tested, which indicated that PAP protein was involved in the differentiation of chromoplasts in sweet orange (Zeng et al., 2015). The results of transgenic studies also confirmed that *PAP* was important for chromoplast development and carotenoid accumulation. The chloroplast ultrastructure in leaves and chromoplast ultrastructure in petals of transgenic *Nicotiana tabacum* plants, which was overexpressing *fibrillin/PAP,* had changed significantly, especially in the number and distribution of plastoglobules (Rey et al., 2000). In tomato, as the pepper *fibrillin/PAP* gene overexpressed, the structure of the chromoplast was greatly affected, leading to a two-fold increase in carotenoid contents (Simkin et al., 2007). Moreover, Leitner-Dagan et al., (2006) found that the flowers of RNAi-transgenic lines with suppressed *LeCHRC* accumulated approximately 30% less carotenoids than controls. Our findings revealed that the expression levels of *CmPg-1*, *CmPAP10* and *CmPAP13* were much higher in JlxY and JlxR, which were capable of transforming chromoplasts and formed a large number of plastoglobules, compared with JlxW and JlxP. In conclusion, *CmPg-1*, *CmPAP10* and *CmPAP13*, which was belonged to subfamiliy 2, 7 and 8 respectively (Fig. S4), may be other key genes in addition to *CmLCYE* and *CmCCD4a-2* in chrysanthemum that can affect carotenoid accumulation by promoting the transformation of chromoplasts.

4.3. Regulatory network of carotenoid biosynthesis and accumulation in chrysanthemum

The genetic regulation of carotenoid metabolism in higher plants has always been popular and difficult to study in the field of secondary metabolism research. Currently, transcription factors related to carotenoid metabolism, which were reported in model plants and crops, are mainly distributed in the MYB, bHLH, MADS-box, NAC transcription factor families. For example, the MYB transcription factor CrMYB68 in citrus can affect carotenoid accumulation by directly inhibiting expression of *CrBCH2* and *CrNCED5* genes (Zhu et al., 2017). In tobacco, nectar contained a large amount of β-carotene due to the high expression of *MYB305*, while β-carotene were not accumulated in nectar while *MYB305* expression was silenced (Liu et al., 2009). This result proved that *NtMYB305* could affect carotenoid synthesis, and *CmMYB305* (TRINITY_DN48859_c0_g1), which we screened out was highly homologous with *NtMYB305*, suggesting that it might also affect carotenoid accumulation in chrysanthemum. Another *MYB* gene, *CmMYB29*, encoding a typical R2R3 MYB transcription factor, also had a similar expression pattern to *CmMYB305*, and its transcriptional level was also significantly correlated with dynamic changes of total carotenoids ($R^2 = 0.9075$). RAD was a type of important MYB transcription factor that determined flower symmetry. RAD1 in *Torenia fournieri* could influence the expression of the *MYB1* gene in the dorsal petal, which inhibited the anthocyanin biosynthesis (Su et al., 2017). We found that the expression pattern of *CmRAD3* was significantly correlated with dynamic changes of total carotenoids in chrysanthemum. Furthermore, we have identified the promoters of the key structural genes (*CmLCYE* and *CmCCD4a-2*) by Takara genome walking kit and found a great number of *cis* elements such as MYB-binding sites, bHLH-binding sites in promoters according to PlantCARE analysis (unpublish data). It indicated that these MYB transcription factor including *CmMYB305, CmMYB29* and *CmRAD3* might regulate the carotenoid metabolism through binding the promoters of *CmLCYE* and *CmCCD4a-2* directly.

Most members of the MADS-box transcription factor family play an important role in the development of plant reproductive organs, including controlling flower development, flowering time regulation, and fruit ripening. Additionally, the MADS-box transcription factor is also involved in carotenoid metabolism. *CsMADS6* isolated from citrus transformed into tomato significantly increased the carotenoid contents of tomato sepals. Electrophoretic mobility shift assay (EMSA) showed that CsMADS6 directly bound to the promoters of *LCYb1, PSY, PDS* and *CCD1* to activate the carotenoid metabolic pathway (Lu et al., 2018). In the present study, we identified a MADS-box transcription factor gene *CmAGL24*, which was the ortholog of the *AtAGL24* in Arabidopsis. AtAGL24 was a very important factor controlling flowering that can interact with other MADS-box transcription factors to activate *LEAFY,* promoting flowering (https://www.frontiersin.org/articles/10.3389/fpls.2016.00823/full, Lee et al., 2008; https://www.frontiersin.org/articles/10.3389/fpls.2016.00823/full, Liu et al., 2008). NAC transcription factors are also involved in regulating carotenoid biosynthesis. Two NAC transcription factors, CpNAC1 and CpNAC2, which were found in papaya, directly bound to the promoters of structural genes to regulate carotenoid biosynthesis. CpNAC1 bound to the NACBS sequence on the *CpPDS2/4* genes' promoters, which resulted in initiating *CpPDS2/4* gene expression, and CpNAC2 interacted with CpEIN3a to

activate the expression of downstream structural genes *CpPDS2/4, CpLCYE* and *CpCHYB* (Fu et al., 2014, 2016). Using correlation analysis, we found that *CmNAC1,* which was located at the center of the gene expression regulatory network, had the highest correlation with the dynamic changes of carotenoids ($R^2 = 0.9717$), and expressed higher in JlxY and JlxR than JlxW and JlxP (Fig. S6). Sequence alignment revealed that it was highly homologous to *AtNAC1,* which promoted root growth through the auxin pathway (Xie et al., 2000). Thus we speculated that this gene might be involved in the metabolic regulation of carotenoids through affecting the auxin signal in chrysanthemum.

The reported transcription factors mentioned above affected carotenoid accumulation by regulating structural genes related to the carotenoid metabolic pathway. Recently, Zhang et al., (2016) found that the differentially expressed chromoplast phosphate transporter gene *ClPHT4;*2 might be the cause of the differential accumulation of carotenoids in white-flesh watermelon cultivar '97103' and red-flesh cultivar 'PI296341FR' through comparative transcriptome analysis. Furthermore, the upstream bZIP transcription factor *ClATB2* contributed to the differential expression of *ClPHT4;2* (Zhang et al., 2016). In this study, we also found that *CmbZIP61,* the homologous gene of *ClATB2,* showed high correlation with carotenoid contents, which indicateed the similar regulation mechanism that affected carotenoid accumulation in chrysanthemum by regulating the expression of genes related to chromoplast development.

5. Conclusions

Using comparative transcriptome analysis combined with gene expression analysis, we found that *CmLCYE* involved in carotenoid biosynthesis, *CmCCD4a-2* involved in carotenoid degradation and *CmPg-1, CmPAP10, CmPAP13* involved in chromoplast transformation were differentially expressed in four cultivars, suggesting that they affected carotenoid accumulation together. In addition, *CmMYB305, CmMYB29, CmRAD3, CmbZIP61, CmAGL24, CmNAC1* transcription factors related to carotenoids were screened out by WGCNA combined with correlation analysis, which could affect the accumulation of chrysanthemum carotenoids by regulating genes involved in the metabolism pathway and plastid development.

Author contributions

HH and SLD conceived and designed this study. CFL, YP and YTL performed the experiments. CFL, JPQ and YJL carried out the data analysis. CFL and HH wrote this manuscript. All authors read and approved the final manuscript.

Acknowledgments

This work was supported by the Beijing Natural Science Foundation, China (grant no. 6172025), National Natural Science Foundation of China, China (grant no. 31501793) and the World-Class Discipline Construction and Characteristic Development Guidance Funds for Beijing Forestry University (2019XKJS0323) is supported by the Chinese Ministry of Education.

Appendix A. Supplementary data

Supplementary data to this article can be found online at https://doi.org/10.1016/j.plaphy.2019.07.023.

References

Bai, X.X., Hu, K., Dai, S.L., Wang, L.S., 2006. Components of flower pigments in the petals of different color *Chrysanthemum morifolium* Ramat. cultivars. J. Beijing Fore. Univ. 28, 84–89 (in Chinese).

Bruno, M., Hofmann, M., Vermathen, M., Alder, A., Beyer, P., Al-Babili, S., 2014. On the substrate-and stereospecificity of the plant carotenoid cleavage dioxygenase 7. FEBS lett. 588 (9), 1802–1807.

Chiu, L.W., Zhou, X., Burke, S., Wu, X., Prior, R.L., Li, L., 2010. The purple cauliflower arises from activation of a MYB transcription factor. Plant Physiol. 154, 1470–1480.

Feng, G., Huang, L., Li, J., Wang, J., Xu, L., Pan, L., Zhao, X., Wang, X., Huang, T., Zhang, X., 2017. Comprehensive transcriptome analysis reveals distinct regulatory programs during vernalization and floral bud development of orchardgrass (*Dactylis glomerata* L.). BMC Plant Biol. 17, 216–234.

Fu, X., Kong, W., Peng, G., Zhou, J., Azam, M., Xu, C., Grierson, D., Chen, K., 2012. Plastid structure and carotenogenic gene expression in red- and white-fleshed loquat (*Eriobotrya japonica*) fruits. J. Exp. Bot. 63, 341–354.

Fu, J.X., Qi, S., Yang, L.W., Dai, Y., Dai, S.L., 2014. Characterization of chrysanthemum *ClSOC1-1* and *ClSOC1-2*, homologous genes of *SOC1*. Plant Mol. Biol. Report. 32, 740–749.

Fu, C.C., Han, Y.C., Fan, Z.Q., Chen, J.Y., Chen, W.X., Lu, W.J., Kuang, J.F., 2016. The papaya transcription factor *CpNAC1* modulates carotenoid biosynthesis through activating phytoene desaturase genes *CpPDS2/4* during fruit ripening. J. Agric. Food Chem. 64, 5454–5463.

Han, Y.J., Wang, X.H., Chen, W.C., Dong, M.F., Yuan, W.J., Liu, X., Shang, F.D., 2014. Differential expression of carotenoid-related genes determines diversified carotenoid coloration in flower petal of *Osmanthus fragrans*. Tree Genet. Genomes 10, 329–338.

Hong, Y., Tang, X.J., Huang, H., Zhang, Y., Dai, S.L., 2015. Transcriptomic analyses reveal species-specific light-induced anthocyanin biosynthesis in chrysanthemum. BMC Genomics 16, 202–220.

Kato, M., Ikoma, Y., Matsumoto, H., Sugiura, M., Hyodo, H., Yano, M., 2004. Accumulation of carotenoids and expression of carotenoid biosynthetic genes during maturation in Citrus fruit. Plant Physiol. 134, 824–837.

Kilambi, H.V., Manda, K., Rai, A., Charakana, C., Bagri, J., Sharma, R., Sreelakshmi, Y., 2017. Green-fruited *Solanum habrochaites* lacks fruit-specifc carotenogenesis due to metabolic and structural blocks. J. Exp. Bot. 68, 4803–4819.

Kishimoto, S., Maoka, T., Nakayama, M., Ohmiya, A., 2004. Carotenoid composition in petals of chrysanthemum (*Dendranthema grandiflorum* (Ramat.) Kitamura). Phytochemistry 65, 2781–2787.

Kishimoto, S., Ohmiya, A., 2006. Regulation of carotenoid biosynthesis in petals and leaves of chrysanthemum (*Chrysanthemum morifolium*). Physiol. Plant. 128, 436–447.

Kishimoto, S., Sumitomo, K., Yagi, M., Nakayama, M., Ohmiya, A., 2007. Three routes to orange petal colour via carotenoid component in 9 compositae species. J. Jpn. Soc. Hortic. Sci. 76, 250–257.

Kim, J.E., Rensing, K.H., Douglas, C.J., Cheng, K.M., 2010. Chromoplasts ultrastructure and estimated carotene content in root secondary phloem of different carrot varieties. Planta 23, 549–558.

Lado, J., Zacarías, L., Gurrea, A., Page, A., Stead, A., Rodrigo, M.J., 2015. Exploring the diversity in citrus fruit colouration to decipher the relationship between plastid ultrastructure and carotenoid composition. Planta 242, 645–661.

Leitner-Dagan, Y., Ovadis, M., Shklarman, E., Elad, Y., David, D.R., Vainstein, A., 2006. Expression and functional analyses of the plastid lipid-associated protein CHRC suggest its role in chromoplastogenesis and stress. Plant Physiol. 142, 233–244.

Lee, J., Oh, M., Park, H., Lee, I., 2008. SOC1 translocated to the nucleus by interaction with AGL24 directly regulates *LEAFY*. Plant J. 55, 832–843.

Li, L., Yuan, H., 2013. Chromoplast biogenesis and carotenoid accumulation. Arch. Biochem. Biophys. 539, 102–109.

Liu, C., Chen, H., Er, H.L., Kumar, P.P., Han, J.H., Liou, Y.C., Yu, H., 2008. Direct interaction of AGL24 and SOC1 integrates flowering signals in Arabidopsis. Development 135, 1481–1491.

Liu, G., Ren, G., Guirgis, A., Thomburg, R.W., 2009. The *MYB305* transcription factor regulates expression of nectarin genes in the ornamental tobacco floral nectary. Plant Cell 21, 2672–2687.

Liu, H., Kishimoto, S., Yamamizo, C., Fukuta, N., Ohmiya, A., 2013. Carotenoid accumulations and carotenogenic gene expressions in the petals of *Eustoma grandiflorum*. Plant Breed. 132 (4), 417–422.

Lu, S., Van, EckJ., Zhou, X., Lopez, A.B., O'Halloran, D.M., Cosman, K.M., Conlin, B.J., Paolillo, D.J., Garvin, D.F., Vrebalov, J., 2006. The cauliflower *or* gene encodes a DnaJ cysteine-rich domain-containing protein that mediates high levels of β-carotene accumulation. Plant Cell 18, 3594–3605.

Lu, S., Li, L., 2008. Carotenoid metabolism: biosynthesis, regulation, and beyond. J. Integr. Plant Biol. 50, 778–785.

Lu, S.W., Zhang, Y., Zhu, K., Yang, W., Ye, J.L., Chai, L., Xu, Q., Deng, X.X., 2018. The citrus transcription factor *CsMADS6* modulates carotenoid metabolism by directly regulating carotenogenic genes. Plant Physiol. 176, 2657–2676.

Martel, C., Vrebalov, J., Tafelmeyer, P., Giovannoni, J.J., 2011. The tomato MADS-box transcription factor RIPENING INHIBITOR interacts with promoters involved in numerous ripening processes in a COLORLESS NONRIPENING-dependent manner. Plant Physiol. 157, 1568–1579.

Mortazavi, A., Williams, B.A., McCue, K., Schaeffer, L., Wold, B., 2008. Mapping and quantifying mammalian transcriptomes by RNA-Seq. Nat. Methods 5, 621–628.

Nazia, N., Li, L., Lu, S., Khin, N., Pogson, B., 2015. Carotenoid metabolism in plants. Mol. Plant 6, 68–82.

Nisar, N., Li, L., Lu, S., Khin, N.C., Pogson, B.J., 2015. Carotenoid metabolism in plants. Mol. Plant 8, 68–82.

Ohmiya, A., Kishimoto, S., Aida, R., Yoshioka, S., Sumitomo, K., 2006. Carotenoid cleavage dioxygenase (*CmCCD4a*) contributes to white color formation in chrysanthemum petals. Plant Physiol. 142, 1193–1201.

Ohmiya, A., Toyoda, T., Watanabe, H., Emoto, K., Hase, Y., Yoshioka, S., 2012. Mechanism behind petal color mutation induced by heavy-ion-beam irradiation of recalcitrant chrysanthemum cultivar. J. Jpn. Soc. Hortic. Sci. 81 (3), 269–274.

Ohmiya, A., Tanase, K., Hirashima, M., Yamamizo, C., Yagi, M., 2013. Analysis of

carotenogenic gene expression in petals and leaves of carnation (*Dianthus caryophyllus* L.). Plant Breed. 132 (4), 423–429.
Park, C.H., Chae, S.C., Park, S.Y., Kim, J.K., Kim, Y.J., Chung, S.O., Arasu, M.V., Al-Dhabi, N.A., Park, S.U., 2015. Anthocyanin and carotenoid contents in different cultivars of chrysanthemum (*Dendranthema grandiflorum* Ramat.) flower. Molecules 20, 11090–11102.
Pan, Z., Zeng, Y., An, J., Ye, J., Xu, Q., Deng, X., 2012. An integrative analysis of transcriptome and proteome provides new insights into carotenoid biosynthesis and regulation in sweet orange fruits. J. Proteomics 75, 2670–2684.
Pogson, B.J., Rissler, H.M., 2000. Genetic manipulation of carotenoid biosynthesis and photoprotection. Philos. Trans. R. Soc. Lond. B Biol. Sci. 355, 1395–1403.
Rey, P., Gillet, B., Römer, S., Eymery, F., Massimino, J., Peltier, G., Kuntz, M., 2000. Overexpression of a pepper plastid lipid-associated protein in tobacco leads to changes in plastid ultrastructure and plant development upon stress. Plant J. 21, 483–494.
Rojas-Garbanzo, C., Gleichenhagen, M., Heller, A., Esquivel, P., Schulze-Kaysers, N., Schieber, A., 2017. Carotenoid profile, antioxidant capacity, and chromoplasts of pink guava (*Psidium guajava* L. Cv.'Criolla') during fruit ripening. J. Agric. Food Chem. 65, 3737–3747.
Simkin, A.J., Gaffé, J., Alcaraz, J.P., Carde, J.P., Bramley, P.M., Fraser, P.D., Kuntz, M., 2007. Fibrillin influence on plastid ultrastructure and pigment content in tomato fruit. Phytochemistry 68, 1545–1556.
Su, L., Diretto, G., Purgatto, E., Danoun, S., Zoulne, M., Li, Z.G., Roustan, J.P., Bouzayan, M., Gluliano, G., Chervin, C., 2015. Carotenoid accumulation during tomato fruit ripening is modulated by the auxin-ethylene balance. BMC Plant Biol. 15, 114–125.
Su, S., Xiao, W., Guo, W., Yao, X., Xiao, J., Ye, Z., Wang, N., Jiao, K., Lei, M., Peng, Q., Hu, X., Huang, X., Luo, D., 2017. The CYCLOIDEA–RADIALIS module regulates petal shape and pigmentation, leading to bilateral corolla symmetry in *Torenia fournieri* (Linderniaceae). New Phytol. 215, 1582–1593.
Sun, W., Li, C., Wang, L., Dai, S.L., 2010. Analysis of anthocyanins and flavones in different-colored flowers of chrysanthemum. Bull. Bot. 45, 327–336 (in Chinese).
Toledo-Ortiz, G., Huq, E., Rodriguez-Concepcion, M., 2010. Direct regulation of phytoene synthase gene expression and carotenoid biosynthesis by phytochrome-interacting factors. Proc. Natl. Acad. Sci. U.S.A. 107, 11626–11631.
Vrebalov, J., Ruezinsky, D., Padmanabhan, V., Whitem, R., Medrano, D., Drake, R., Schuch, W., Giovannoni, J., 2002. A MADS-box gene necessary for fruit ripening at the tomato ripening-inhibitor (rin) locus. Science 296, 343–346.
Wang, Z., Meng, D., Wang, A., Li, T., Jiang, S., Cong, P., Li, T., 2013. The methylation of the *PcMYB10* promoter is associated with green-skinned sport in Max Red Bartlett pear. Plant Physiol. 162, 885–896.
Wisutiamonkul, A., Ampomah-Dwamena, C., Allan, A.C., Ketsa, S., 2017. Carotenoid accumulation in durian (*Durio zibethinus*) fruit is affected by ethylene via modulation of carotenoid pathway gene expression. Plant Physiol. Biochem. (Montrouge) 115, 308–319.
Wu, J., Zhang, Y., Zhang, H., Huang, H., Folta, K., Lu, J., 2010. Whole genome wide expression profiles of *Vitis amurensis* grape responding to downy mildew by using Solexa sequencing technology. BMC Plant Biol. 10, 234–249.
Xiang, L.L., Liu, X.F., Li, X., Yin, X.R., Grierson, D., Li, F., Chen, K.S., 2015. A novel bHLH transcription factor involved in regulating anthocyanin biosynthesis in Chrysanthemums (*Chrysanthemum morifolium* Ramat.). PloS One 10 (11), e0143892.
Xie, Q., Frugis, G., Colgan, D., Chua, N.H., 2000. Arabidopsis *NAC1* transduces auxin signal downstream of TIR1 to promote lateral root development. Genes Dev. 14, 3024–3036.
Yang, J., Yu, H., Liu, B.H., Zhao, Z.M., Liu, L., Ma, L.X., Li, Y.X., Li, Y.Y., 2013. DCGL v2.0: an R package for unveiling differential regulation from differential co-expression. PLoS One 8, e79729.
Yang, T., Li, K., Hao, S., Zhang, J., Song, T., Tian, J., Yao, Y., 2018. The use of RNA sequencing and correlation network analysis to study potential regulators of leaf color transformation. Plant Cell Physiol. 59, 1027–1042.
Yamamizo, C., Kishimoto, S., Ohmiya, A., 2009. Carotenoid composition and carotenogenic gene expression during Ipomoea petal development. J. Exp. Bot. 61 (3), 709–719.
Yoshioka, S., Aida, R., Yamamizo, C., Shibata, M., Ohmiya, A., 2012. The carotenoid cleavage dioxygenase 4 (*CmCCD4a*) gene family encodes a key regulator of petal color mutation in chrysanthemum. Euphytica 184 (3), 377–387.
Zeng, Y., Du, J., Wang, L., Pan, Z., Xu, Q., Xiao, S., Deng, X., 2015. A comprehensive analysis of chromoplast differentiation reveals complex protein changes associated with plastoglobule biogenesis and remodelling of protein systems in orange flesh. Plant Physiol. 168, 1648–1665.
Zhan, J.P., Thakare, D., Ma, C., Lloyd, A., Nixon, N.M., Arakaki, A.M., Burnett, W.J., Logan, K.O., Wang, D., Wang, X., Drews, G.N., Yadegari, R., 2015. RNA sequencing of laser-capture microdissected compartments of the maize kernel identifies regulatory modules associated with endosperm cell differentiation. Plant Cell 27, 513–531.
Zhang, J., Guo, S., Ren, Y., Zhang, H., Gong, G., Zhou, M., Wang, G., Zong, M., He, H., Liu, F., 2016. High-level expression of a novel chromoplast phosphate transporter *ClPHT4;2* is required for flesh color development in watermelon. New Phytol. 3, 1208–1221.
Zhou, X.R., Wang, Y.Z., Smith, J.F., Chen, R., 2008. Altered expression patterns of TCP and MYB genes relating to the floral developmental transition from initial zygomorphy to actinomorphy in Bournea (Gesneriaceae). New Phytol. 178, 532–543.
Zhu, M., Chen, G., Zhou, S., Tu, Y., Wang, Y., Dong, T., Hu, Z., 2013. A new tomato NAC (N AM/A TAF1/2/C UC2) transcription factor, *SlNAC4*, functions as a positive regulator of fruit ripening and carotenoid accumulation. Plant Cell Physiol. 55, 119–135.
Zhu, F., Luo, T., Liu, C., Wang, Y., Yang, H., Yang, W., Zheng, L., Xiao, X., Zhang, M., Xu, R., Xu, J., Zeng, Y., Xu, J., Xu, Q., Guo, W., Larkin, R.M., Deng, X., Cheng, Y., 2017. An R2R3-MYB transcription factor represses the transformation of α-and β-branch carotenoids by negatively regulating expression of *CrBCH2* and *CrNCED5* in flavedo of *Citrus reticulate*. New Phytol. 216, 178–192.